Group A *Streptococcus* Induces Lysosomal Dysfunction in THP-1 Macrophages

Scott T. Nishioka[1†], Joshua Snipper[1†], Jimin Lee[1], Joshua Schapiro[1], Robert Z. Zhang[1], Hyewon Abe[1], Andreas Till[2,3], Cheryl Y.M. Okumura[1*]

[1]Biology Department, Occidental College, Los Angeles, CA 90041, USA

[2]Division of Biological Sciences and The San Diego Center for Systems Biology, University of California San Diego, La Jolla, CA 92093-0688, USA

[3]University Hospital of Bonn, Bonn, Germany

[†]These authors have contributed equally to this work and share first authorship

*** Correspondence:**
Cheryl Okumura
okumura@oxy.edu

Keywords: Group A *Streptococcus*, streptolysin O (SLO), macrophage, lysosome, vacuolar ATPase, cathepsin B

Abstract

The human-specific bacterial pathogen Group A *Streptococcus* (GAS) is a significant cause of morbidity and mortality. Macrophages are important to control GAS upon infection, but previous data indicate that GAS can persist in macrophages. In this study, we detail the molecular mechanisms by which GAS survives in THP-1 macrophages. Our fluorescence microscopy studies demonstrate that GAS are readily phagocytosed by macrophages, but persist within phagolysosomes. These phagolysosomes are not acidified, which is in agreement with the inability of the GAS to survive in low pH environments. We find that the secreted pore-forming toxin Streptolysin O (SLO) perforates the phagolysosomal membrane, allowing leakage of not only protons, but large proteins including the lysosomal protease cathepsin B. Additionally, GAS blocks the activity of vacuolar ATPase (v-ATPase) to prevent acidification of the phagolysosome. Thus, while GAS does not inhibit fusion of the lysosome with the phagosome, it has multiple mechanisms to prevent proper phagolysosome function, allowing for persistence of the bacteria within the macrophage. This has important implications for not only the initial response, but the overall function of the macrophages and resulting pathology in GAS infection and suggests that therapies aimed at improving macrophage function may improve outcomes in GAS infection.

1 Introduction

GAS is a significant cause of morbidity and mortality worldwide, but especially in medically underserved areas where antibiotic therapy may not be promptly available (1). Infection produces wide-ranging clinical manifestations including pharyngitis, acute rheumatic fever (ARF) often leading to rheumatic heart disease, and invasive disease such as necrotizing fasciitis (1). Acting as the first line of defense against such infections, macrophages are critical for the early control and resolution of GAS infection (2,3). However, GAS has been shown to survive intracellularly in macrophages during both acute invasive soft tissue infection and asymptomatic carriage (3–5). Although GAS remains highly sensitive to beta-lactam antibiotics, the gold standard of treatment (6),

the ability of bacteria to persist in macrophages and re-emerge after antibiotic treatment poses a therapeutic challenge (4).

As both phagocytes and antigen-presenting cells, macrophages function at the intersection of innate and adaptive immunity and are therefore critical for identifying and defending against infection. Macrophages engulf bacterial pathogens into phagosomes, which fuse with lysosomes that deliver proteolytic enzymes to facilitate bacterial destruction. These enzymes have optimal proteolytic activity under acidic conditions, and therefore lysosomal acidification is important for macrophage bactericidal function and subsequent antigen presentation (7). Inhibition of either lysosomal fusion with bacteria-containing phagosomes or phagolysosomal acidification is an evasion tactic employed by several bacterial pathogens including *Mycobacterium tuberculosis*, *Legionella pneumophila*, and *Staphylococcus aureus* (7–9). GAS may employ similar tactics to survive intracellularly within macrophages and to evade the adaptive immune response upon host re-infection, which may contribute to the development of pathologies such as toxic shock syndrome (10).

GAS is a human-specific pathogen and therefore has evolved mechanisms to survive the immune response (11). Previous data have indicated that phagocytosed GAS can prevent fusion with destructive organelles such as azurophilic granules and lysosomes (12,13). Other reports have shown that while GAS-containing phagosomes do fuse with lysosomes, GAS survives within macrophages via the secretion of virulence factors such as Streptolysin O (SLO) and NADase (14,15). SLO is a cholesterol-dependent cytolysin that oligomerizes to form large pores (~25-30 nm) within the host cell membrane (16). As a result, SLO is hypothesized to permeabilize the phagolysosomal membrane, permitting free flow of protons out of the phagolysosome and limiting the activity of lysosomal proteases that facilitate intracellular killing (15,17). Interestingly, it has also been reported that GAS is capable of preventing lysosomal acidification by preventing the recruitment of the vacuolar ATPase (v-ATPase) (18). In the context of these data, it is unclear what mechanisms are contributing to GAS intracellular survival in macrophages. In this paper, we used the human monocytic cell line THP-1 differentiated into macrophages to understand the molecular mechanism by which GAS survives in macrophages. We find that not only does GAS induce leakage of large proteins from the phagolysosome into the cytosol, but that acidification of the phagolysosome is also limited. This has important consequences for the survival of the bacteria within the macrophage and underscores the need to mount a proper macrophage response in GAS infection to improve patient outcomes.

2 Materials and Methods

2.1 Antibodies and chemicals

Antibodies to the following proteins were used in this study: EEA-1 (Abcam, ab2900), LAMP-2 (Abcam, ab25631), V_0D_1 (Abcam, ab56441), Cathepsin B (Cell Signaling Technology, D1C7Y), LAMP-1 (Cell Signaling Technology, #9091), V_1A (Abnova, H00000523-A01), and beta-actin (Thermo Fisher Scientific, MA5-15739). Fluorescent secondary antibodies were purchased from Thermo Fisher Scientific. The following fluorescent probes were purchased from Thermo Fisher Scientific: Alexa Fluor 488 Hydrazide (A10436), Oregon Green 488 Anionic, Lysine Fixable Dextran,10,000 MW (D7171) and 70,000 MW (D7173), and LysoTracker DeepRed (L12492). 40,000 and 70,000 MW Fluorescein isothiocyanate (FITC) dextrans were purchased from Millipore Sigma. To generate antibody-coupled beads, 0.1um Carboxylate-Modified Microspheres (Thermo Fisher Scientific) were coupled to approximately 400mg normal pooled human serum (Thermo

84 Fisher Scientific) using 2% 1-Ethyl-3-(3-dimethylaminopropyl) carbodiimide hydrochloride
85 (QBiosciences). The reaction was quenched with 40mM ethanolamine and resuspended in PBS.
86 Successful coupling of the beads was assessed by fluorescence microscopy and increased
87 phagocytosis by THP-1 macrophages compared with uncoupled beads (data not shown). 1mM L-
88 leucyl L-leucine O-methyl ester (LLOMe, Cayman Chemical, #16008) was incubated with cells to
89 induce lysosomal damage.

90 **2.2 Bacterial strains**

91 Wild-type (WT) GAS strain M1T1 5448 (M1 GAS) was originally isolated from a patient with
92 necrotizing fasciitis and toxic shock syndrome (19). Isogenic mutant strains lacking Streptolysin O
93 (ΔSLO), Streptolysin S (via lack of SagA, ΔSagA) and Emm1 (ΔM1) were previously described (20–
94 22). Bacterial strains were cultivated in Todd-Hewitt broth (THB) at 37˚C. For all experiments,
95 bacteria were grown to log phase in the presence of 1:200 pooled normal human serum (Thermo
96 Fisher Scientific) to opsonize bacteria. The gene for monomeric WASABI (mWASABI) (23,24) was
97 codon-optimized for expression in bacteria and synthesized in a shuttle vector (GenScript; see
98 supplemental data for amino acid sequence). The gene was subcloned into pDCerm (25) and the
99 resulting plasmid (pWASABI) was transformed into WT M1 GAS and the ΔSLO mutant. Plasmid-
100 bearing strains were maintained in THB supplemented with 5ug/mL erythromycin. Heat-killed (HK)
101 bacteria were prepared by incubating a known concentration of bacteria at 95°C for 10 min. followed
102 by a 15 min. opsonization in 1:200 pooled normal human serum at room temperature.

103 **2.3 Cell Culture**

104 THP-1 cells were purchased from Sigma (cat. 88081201) and cultured in RPMI supplemented with
105 10% heat inactivated fetal bovine serum (FBS) (Corning), 2mM L-glutamine and 100 U/mL
106 penicillin/100 µg/mL streptomycin at 37°C/5% CO_2. Cells were differentiated to macrophages using
107 20nM phorbol 12-myristate 13-acetate (PMA) (MilliporeSigma) 24-48 hours prior to experiments.

108 **2.4 Immunofluorescence**

109 2.5 x 10^5 THP-1 cells were seeded on coverslips in the presence of 20nM PMA 24-48 hours prior to
110 experiments. For dextran leakage assays, cells were incubated in media containing 20ug/mL of the
111 indicated dextran or 500ug/mL 70kD dextran overnight, washed and chased in cell culture media for
112 2 hours prior to bacterial infection. Bacteria were combined with cells at an MOI = 10 in RPMI
113 supplemented with 2% FBS only (no antibiotics). At the indicated time points, cells were fixed with
114 4% paraformaldehyde or 3.7% formaldehyde for 10 min. at room temperature. Cells were incubated
115 with blocking solution (10% goat serum, 3% BSA and 0.1% Triton X-100 in PBS), then incubated
116 with the indicated primary antibodies for 1 hour at room temperature in block solution. Cells were
117 washed and incubated with the indicated secondary antibodies for 1 hour at room temperature. Cells
118 were washed and mounted onto slides with ProLong antifade reagent with DAPI (Thermo Fisher
119 Scientific). Slides were imaged on an inverted Leica TCS SP5 confocal microscope using a 63x/1.40
120 oil objective with 2-3x digital zoom at calibrated magnifications and recorded with LAS AF software
121 (Leica). Quantitation of dextran and LAMP-1 colocalization with bacteria was analyzed with
122 CellProfiler 3.1.9 (26) using the Otsu thresholding method. For dextran, colocalization is expressed
123 as the percentage of dextran-labeled lysosomes that colocalized with bacteria compared with the total
124 number of lysosomes. For LAMP-1, colocalization is expressed as the percentage of LAMP-1 that
125 colocalized with bacteria compared with the total number of bacteria. For quantitation of GFP-
126 expressing bacteria within phagosomes, images were coded and counted manually in a blind fashion
127 by at least 4 independent reviewers. For all imaging data, at least 3 independent experiments were

128 performed, at least 16 images containing >10 cells per image were analyzed and at least 100 cells
129 were counted per time point.

130 **2.5 Verification of pH sensitivity of mWASABI in GAS**

131 To assess the fluorescence intensity of mWASABI in live GAS, log phase cultures of bacteria were
132 incubated on coverslips in THB with 10mM HEPES adjusted to the indicated pH for 1 hour at 37°C.
133 Bacteria were fixed with 2% paraformaldehyde and analyzed by confocal microscopy. Gain settings
134 were adjusted to bacteria incubated in pH 7 media, and the same settings were applied to all other
135 conditions. Images were thresholded and the corrected total cell fluorescence (integrated density –
136 average background integrated density) of each bacterial cell was measured using ImageJ.

137 **2.6 Acidification assay**

138 10^5 THP-1 cells were seeded with 20nM PMA in 96-well black plates with clear bottoms overnight.
139 Cells were fed 500ug/mL 70kD FITC-dextran overnight. The following day, cells were chased with
140 normal cell culture media for 2 hours prior to infection. Cells were infected at an MOI of 10 with
141 either the indicated bacterial strain or Ab-conjugated latex beads. Fluorescence intensity at
142 480nm/535nm (Em/Ex) was monitored at 37°C in a fluorescent plate reader every 15 min. for 3
143 hours.

144 **2.7 Bacterial survival in different pH media**

145 Bacteria were incubated in THB with 10mM HEPES adjusted to the indicated pH. For bacterial
146 growth, cultures were adjusted to an OD_{600nm} of 0.1 and incubated at 37°C. OD_{600nm} was measured
147 every 15 min. For bacterial survival, 2 x 10^5 cfu log phase bacteria were added to 250ul pH-adjusted
148 culture media in 96 well plates. At the indicated time point, a 25ul aliquot was removed from the
149 culture and quantitated by plating on agar plates.

150 **2.8 Cell fractionation and Western blot**

151 Following a 30 min. infection period, a total of 10^7 PMA-differentiated cells were scraped and
152 collected in 1 mL of fractionation buffer (50 mM KCl, 90 mM K-Gluconate, 1 mM EGTA, 5 mM
153 MgCl2, 50 mM sucrose, 20 mM HEPES, pH 7.4, 5 mM glucose, 1X HALT phosphatase/protease
154 inhibitor cocktail (Thermo Fisher Scientific), 1ug/mL pepstatin (Millipore Sigma), and 1mM PMSF
155 (Millipore Sigma)). Cells were lysed by nitrogen cavitation equilibrated on ice for 30 min. at 400 psi.
156 The resulting lysates were fractionated into membrane and cytosolic fractions by centrifugation at
157 16,000 xg at 4˚C for 15 min. (pellet = membrane fraction, supernatant = cytosolic fraction). Protein
158 concentrations were measured by BCA assay (Thermo Fisher Scientific). 10ug of each sample was
159 run on SDS-PAGE gels and transferred to a 0.2um PVDF membrane. Blots were blocked with 5%
160 (w/v) non-fat dry milk in 1X Tris-buffered saline with 0.1% Tween 20 (TBST). Blots were probed
161 with the indicated antibodies overnight at 4˚C. Relative protein concentrations were quantified by
162 densitometry analysis in ImageLab v. 6.0.1 (BioRad). v-ATPase assembly was measured by
163 normalizing V_1A densitometry values in the membrane fraction to the V_0D_1 loading controls (in
164 membrane fractions) and calculating the ratio of V_1A in the sample compared with uninfected
165 macrophages (27).

166 **2.9 Cathepsin B activity assay**

167 4 x 10^6 PMA-differentiated THP-1 cells were infected at an MOI = 10 for 60 min. followed by lysis
168 with 30ug/mL digitonin in acetate buffer (50 mM Na-acetate pH 5.6, 150 mM NaCl, 0.5 mM EDTA)

169 and protease inhibitors (1X HALT phosphatase/protease inhibitor cocktail (Thermo Fisher
170 Scientific), 100 µM PMSF, 1 µg/mL pepstatin)) (28). The cell lysate was separated into cytosolic and
171 membrane fractions as described above. Cathepsin B activity in cytosolic fractions was measured
172 using the SensoLyte 520 Cathepsin B Assay Kit (AnaSpec) according to the manufacturer's
173 instructions. Relative fluorescence units were normalized to the corresponding protein concentration
174 for each sample and compared with the untreated cells. Data from 3 independent experiments were
175 combined.

176 **2.10 v-ATPase activity assay**

177 Cell membrane fractions containing lysosomes were prepared using 30ug/mL digitonin in acetate
178 buffer as described above. 10ug of each sample was equilibrated in 200ul assay buffer (10mM
179 HEPES, 5mM MgCl2, 125mM KCl, pH = 7.0) (29) at room temperature for 30 min. in the presence
180 or absence of 200nM bafilomycin (MilliporeSigma). 1mM fresh ATP in 200mM Tris pH = 7 was
181 added to each sample and incubated at room temperature for 2.5 hours. 25ul of the reaction was
182 collected and diluted in ultrapure water, and liberation of free phosphate was measured using the
183 Malachite Green Phosphate Assay Kit according to the manufacturer's instructions (MilliporeSigma).
184 Corrected absorbance values (= A_{sample} - $A_{substrate\ blank}$ - $A_{buffer\ blank}$) were compared with a phosphate
185 standard curve to determine phosphate concentration. v-ATPase activity was calculated as the
186 difference in phosphate concentration between samples incubated with and without bafilomycin.

187 **2.11 Statistical analysis**

188 Growth curve data was analyzed using the Growthcurver package in R (30) and comparison of the
189 intrinsic growth rate (r) and carrying capacity (K) was analyzed by one-way ANOVA and Tukey's
190 post-hoc test. All other data were analyzed using Prism v. 9.3.1 (GraphPad Software) by one-way
191 ANOVA with Tukey's (normally distributed data) or Kruskal-Wallis (nonparametric data) multiple
192 comparison tests. Outliers were assessed by the ROUT method (Q = 1%). For all data presented,
193 ****P<0.0001, ***P<0.001, *P<0.05, n.s., not significant.

194 **3 Results**

195 **3.1 Bacterial trafficking in THP-1 macrophages**

196 We first wanted to determine the intracellular fate of GAS in THP-1 macrophages. To study
197 bacterial trafficking, we performed a short time course infection experiment with WT M1 GAS and
198 tracked phagolysosomal maturation. In agreement with other reports (13,15,31), bacteria were rapidly
199 engulfed by THP-1 cells within 7.5 minutes (Fig. 1A, B) and colocalized with the phagolysosomal
200 marker EEA-1 (Fig. 2). Interestingly, bacteria in phagosomes began colocalizing with the lysosomal
201 marker LAMP-1 as early as 7.5 minutes, with maximal colocalization at 30 minutes (Fig. 1A, B).
202 GAS remained in phagolysosomes throughout the later time points (Fig. 1B), and the number of
203 bacteria per cell was relatively constant throughout the experiment (Fig. 1C). These data indicated
204 that bacteria were trafficked normally to phagolysosomes, but bacteria were held in these
205 compartments without observable bacterial killing.

206 **3.2 GAS reside in non-acidified phagolysosomes in THP-1 macrophages**

207 Because bacteria appeared to be held in phagolysosomes, we wondered whether
208 phagolysosomes containing GAS were acidified. Acidification is critical for optimal activity of the
209 proteolytic enzymes in the lysosome (32). Lysotracker is an acidotropic dye commonly used to track

210 acidic compartments such as lysosomes in the cell. However, because GAS is an acid-producing
211 bacterial species, we tested whether Lysotracker would be an accurate indicator of lysosomal pH in
212 GAS-infected cells. Although Lysotracker colocalized with lysosomal markers in THP-1 cells, the
213 staining and uptake was inconsistent (Supp. Fig. 1A). Furthermore, bacteria were brightly stained
214 with Lysotracker in both infected cells and in the absence of cells (Supp. Fig. 1A-C). This made it
215 difficult to determine whether and to what extent phagolysosomes containing GAS were acidified.
216 We therefore expressed a pH-sensitive green fluorescent protein variant mWASABI (24) in GAS to
217 monitor phagolysosomal pH of GAS-infected cells (Fig. 2A). Green fluorescence produced by live
218 bacteria was appropriately quenched in low pH environments (Fig. 2A, B). Notably, pH was
219 distinguishable by fluorescence intensity between pH 5.0 and 4.5 (Fig. 2B).

220 We infected THP-1 macrophages with mWASABI-expressing GAS and performed a detailed
221 trafficking assay of GAS through the phagolysosomal pathway (Fig. 2C, D). Because bacteria were
222 tracked by mWASABI expression instead of immunofluorescent staining, we manually counted
223 bacteria that colocalized with phagolysosomal markers (Fig. 2C, D). We again found that GAS was
224 initially located in phagosomes, as indicated by EEA-1 staining, which was followed by rapid
225 bacterial colocalization with the mature lysosomal marker LAMP-2 within 15 minutes of infection
226 (Fig. 2C, D), similar to the colocalization dynamics observed with LAMP-1 staining (Fig. 1). A
227 significant proportion of the total intracellular bacteria were colocalized with LAMP-2 within 60
228 minutes post-infection (Fig. 2C, D). Although there were some fluctuations in the number of bacteria
229 in phagolysosomes (Fig. 2E), the number of intracellular bacteria remained relatively constant at all
230 time points, consistent with our initial data (Fig. 1C). This corroborated our finding that little to no
231 bacterial eradication or replication was occurring within this time frame (Fig. 2E). Surprisingly, we
232 also found that the green fluorescence signal did not diminish over time (Fig. 2C, F). Fluorescence
233 signal intensity of intracellular bacteria in phagolysosomes was not significantly different than that of
234 extracellular bacteria (Fig. 2F). As the lysosomal lumen is typically between pH 4.5–5 when
235 acidified (33), a pH level that our mWASABI probe can differentiate (Fig. 2A, B), these data
236 indicated that GAS were maintained in phagolysosomes that are not appropriately acidified.

237 We confirmed that GAS-infected phagosomes were not acidified with a second method using
238 pH-sensitive FITC-conjugated 70kD dextran particles. Acidification of the lysosomes resulted in
239 quenching of the fluorescence signal in uninfected and control cells infected with immunoglobulin-
240 conjugated beads (Fig. 2G). However, the fluorescence signal was increased in cells infected with all
241 tested strains of GAS, indicating no pH change (Fig. 2G). These results confirmed that GAS-infected
242 phagolysosomes are not properly acidified, which may account for the persistence of the bacteria in
243 THP-1 cells (Fig. 1C, 2E).

244 **3.3 GAS does not tolerate lysosomal acidic conditions**

245 The pH of the lysosomal lumen has been reported to range between pH 4.5-5 (33). Because
246 GAS is a lactic acid-producing bacterial species capable of acidifying its environment and possesses
247 systems such as the arginine deiminase (ADI) pathway that confer acid tolerance (34,35), we
248 wondered whether a pH similar to that found in the lysosome adversely affected bacterial growth and
249 survival. In growth experiments, bacteria grown in media adjusted to pH 5 or lower did not
250 demonstrate measurable growth (Fig. 3A). Bacteria grown in media adjusted to pH 6 grew at a
251 significantly slower rate and did not reach a similar maximum population size in the time frame of
252 our experiment compared with the unbuffered media control (Fig. 3A). Although growth rates were
253 slower, the ability of bacteria to grow in pH 6 media is consistent with the ability of bacteria to grow
254 in increasingly acidified media, as indicated by the final pH of the stationary phase cultures in

255 unbuffered culture media (Table 1). For bacteria grown in buffered media adjusted to pH 7, there was
256 no significant difference in maximum population size, but a statistically significant increase in the
257 intrinsic growth rate of the population compared with unbuffered media (Fig. 3A). Thus, bacterial
258 growth is inhibited by low pH. As expected, we found that the final pH of both buffered and
259 unbuffered culture medium after bacterial growth was acidic (Table 1).
260
261 Quantitative plating of cultures at various time points throughout the growth experiment
262 indicated that bacteria in pH 5 media were present, but not measurably growing (data not shown). We
263 therefore performed a detailed time course to monitor bacterial survival in low pH media (Fig. 3B).
264 Bacteria incubated in unbuffered media did not significantly grow during the time frame of the
265 experiment (data not shown). Similar to other studies (36,37), we found that GAS does not survive in
266 low pH media (Fig. 3B). Although bacteria incubated in up to pH 5.3 media could survive for a short
267 time, bacterial numbers declined at later time points (Fig. 3B), in agreement with pH 5 being the limit
268 at which bacteria can survive (35,38) and the final pH of bacteria grown in media (Table 1).
269 Combined, our data affirm that GAS cannot survive in the acidified lysosome. Thus, in order to
270 persist in the phagolysosome, GAS likely prevents its acidification.
271

272 **3.4 Streptolysin O creates large perforations in the phagolysosome**

273 Although GAS has several acid stress response strategies, a better tactic may be to avoid the
274 acidification of the phagolysosome altogether (39). The inability of bacteria to survive in low pH
275 environments (Fig. 3) led us to examine whether GAS infection has a mechanism to prevent
276 phagolysosomal acidification. Pore-forming toxins such as SLO create pores as large as 25-30nm in
277 size (16). Streptolysin S (SLS) can similarly perforate membranes (40). Others have shown that pore-
278 forming toxins, including SLO, allow escape of hydrogen ions that prevent acidification of the
279 lysosome (15,41). To confirm these data, we fed THP-1 macrophages fluorescent-conjugated
280 molecules and dextrans of various sizes to assess pore size and leakage from phagolysosomes in
281 GAS-infected cells. The ability to measure phagosomal leakage was confirmed using a fluorescent
282 dye approximately 570Da in size, a 10kD dextran and the lysosomal permeabilization agent LLOMe
283 (Supp. Fig. 2A). LLOMe permeabilizes lysosomes to molecules up to at least 4.4KDa, but not to
284 molecules greater than 10kD (28). Retention of the 10kD, but not the 570Da probe in LLOMe-treated
285 cells confirmed uptake of the probe in phagolysosomes and appropriate release into the cytosol upon
286 permeabilization (Supp. Fig. 2A). Cells loaded with probes were infected with various strains of
287 GAS (Fig. 4A, B). As expected, WT GAS caused probes up to 40kD in size, approximately 9nm
288 diameter (42), to leak from phagolysosomes (Fig. 4A, B). ΔSLO GAS-infected cells retained the
289 probes, while cells infected with ΔSagA GAS (lacking SLS) allowed leakage of the probes, similar to
290 the WT strain (Fig. 4A, B). Mutant bacteria lacking the surface protein M1 (ΔM1), but with unaltered
291 expression of SLO and SLS behaved similarly to WT strains (Fig. 4A, B). Heat-killed bacteria (HK)
292 that retain surface structure but are unable to secrete proteins such as SLO and SLS were included as
293 a comparison and corroborated the data from cells infected with the live GAS strains (Fig. 4A, B).
294 Compared with heat-killed bacteria, WT bacteria could retain probes up to 70kD in size
295 (approximately 13nm diameter) in agreement with the literature (42), though it is possible that
296 leakage of probes of this size still occurs (Fig. 4B, compare with ΔSLO). In our assays, SLS did not
297 significantly damage the phagolysosomal membrane, as indicated by the lack of leakage of even the
298 small 570Da probe (Supp. Fig. 2B). These data indicate that SLO is the primary pore-forming toxin
299 that perforates the phagolysosome and allows leakage of not only protons, but relatively large
300 molecules.
301

302 Because such large molecules can leak from GAS-infected phagosomes, we wondered whether
303 lysosomal enzymes could escape into the cytosol through SLO-mediated pores. We infected cells
304 with WT or ΔSLO GAS and collected membrane and cytosolic cell fractions. Lack of lysosomal
305 markers in the cytosolic fraction indicated little to no contamination of the cytosolic fraction with
306 lysosomes (Fig. 2C). The membrane fraction contained the majority of the lysosomal enzyme
307 cathepsin B as expected (Fig. 2C). However, we noted a small, but visible increase in the amount of
308 cathepsin B present in the cytosolic fraction of WT-infected cells compared with uninfected and
309 ΔSLO-infected cells (Fig. 2C). In order to verify that cathepsin B was present in the cytosol, we
310 measured cathepsin B activity in the cytosolic fraction. Cytosolic fractions from WT-infected cells
311 contained the highest amount of cathepsin B activity compared with uninfected cells (Fig. 2D).
312 Cytosolic fractions from ΔSLO bacteria incapable of leaking large proteins from the phagolysosome
313 (Fig. 2B) did not exhibit cathepsin B activity higher than background levels in uninfected cells (Fig.
314 2D). These data confirmed that SLO secreted by WT bacteria perforates the phagolysosomal
315 membrane and allows the leakage of large proteins into the cytosol. This loss of proteolytic enzymes
316 from the phagolysosome likely also contributes to the ability of GAS to persist in the phagolysosome
317 during infection.

318 **3.5 GAS prevents proper function of vacuolar ATPase**

319 Although SLO-mediated pores could cause leakage of protons from the phagolysosome,
320 reports in the literature suggest that the v-ATPase that is required for acidification of the lysosome is
321 non-functional in GAS-infected cells (18). Supporting this, we found that the phagolysosomes of
322 macrophages infected with ΔSLO and heat-killed bacteria were also not acidified (Fig. 2G).
323 Furthermore, ΔSLO bacteria are trafficked to phagolysosomes and are maintained at consistent
324 numbers in THP-1 cells similar to WT bacteria (Supp. Fig. 3), consistent with the idea that
325 phagolysosomes infected with ΔSLO bacteria were not acidified. We therefore investigated whether
326 v-ATPase is properly assembled and functional in GAS-infected cells. v-ATPase consists of the
327 membrane-bound F_0 subunit (containing the V_0D_1 protein) that must assemble with the cytosolic F_1
328 subunit (containing the V_1A) for proper function (27). We monitored v-ATPase assembly by tracking
329 movement of the V_1A subunit from the cytosolic to membrane fractions. Cells fed Ig-conjugated
330 beads (Ab beads) were included as a positive control (Fig. 5A, B). We observed no significant
331 difference in v-ATPase subunit assembly in cells infected with GAS compared to Ab-bead fed or
332 uninfected cells (Fig. 5A, B). This observation was consistent for cells infected with either WT or
333 ΔSLO GAS, as well as heat-killed bacteria (Fig. 5A, B). However, when we measured the v-ATPase
334 activity in membrane fractions of GAS-infected cells, we found significantly decreased v-ATPase
335 activity in fractions from cells infected with all strains of GAS compared with uninfected cells (Fig.
336 5C). These data are in agreement with the lack of acidification in GAS-infected cells (Fig. 2G).
337 Therefore, though the v-ATPase is properly assembled in GAS-infected cells, the activity of this
338 enzyme is decreased, preventing proper acidification of the phagolysosome. Thus, our data suggests
339 that GAS persists in macrophages by employing a multi-pronged approach to avoid the destructive
340 mechanisms of the phagolysosome.

341 **4 Discussion**

342 The human-specific pathogen GAS has co-evolved with the human immune system, and
343 therefore has multiple mechanisms for survival within the host (1,11). Although GAS is an
344 extracellular bacterial pathogen, phagocytic cells such as macrophages can readily engulf bacteria
345 (13,15,31). The ability of GAS to not only survive in macrophages, but to potentially alter their

346 function, escape downstream immune responses, and be sheltered from antibiotic treatment provides
347 a basis for successful persistence in humans.

348 In our experiments, we found that GAS was readily phagocytosed and phagosomes quickly
349 fused with lysosomes, but that GAS remained intact in these compartments (Fig. 1, 2). There is
350 conflicting evidence in the literature about the fusion of lysosomes with GAS-containing phagosomes
351 in macrophages, which may be due to a difference in cell origin or antibodies (13,15). In addition, we
352 corroborated previous data that SLO induces perforation and damage of the phagolysosomal
353 membrane (Fig. 4) (15,43). Although ΔSLO GAS also prevented phagolysosomal acidification (Fig.
354 2, 5), others have shown that ΔSLO GAS are less fit for survival in macrophages and other cells
355 (15,44). ΔSLO GAS is likely still susceptible to other macrophage killing mechanisms such as
356 reactive oxygen species or xenophagy (44). However, all data are in agreement that in macrophages,
357 GAS does not escape into the cytosol and remains in a membrane-bound structure (Fig. 2, Supp. Fig.
358 3) (13,15). In THP-1 macrophages, bacteria do not replicate in this structure, but they are also not
359 eradicated (Fig. 1, 2, Supp. Fig. 3) (31). This is different from what has previously been observed in
360 epithelial cells, where GAS escapes into the cytosol and replicates (14,43). The downstream fate of
361 GAS in non-functional lysosomes in THP-1 macrophages remains to be elucidated.

362 The pH of the lysosomal lumen has been reported to range between pH 4.5-5 (33). However,
363 we found that acidified medium was sufficient to kill GAS (Fig. 3). These results are surprising since
364 not only does GAS produce lactic acid, but previous reports suggest GAS has multiple mechanisms
365 for acid tolerance, including a F_0/F_1 proton pump and the arginine deiminase pathway which
366 produces alkali (34,35,39,45). However, there may be a limit to which these systems work, especially
367 within an enclosed environment such as in vitro conditions or in the phagolysosome, as demonstrated
368 by the threshold for bacterial survival in low pH medium (Fig. 3) (35). Additionally, GAS lacks
369 enzymes such as glutamate decarboxylase and urease (39), making neutralization of highly acidified
370 environments a less viable strategy. Therefore, two mechanisms to prevent acidification, perforating
371 the phagolysosomal membrane (Fig. 4) and blocking v-ATPase activity (Fig. 5) provide a means to
372 survive within the phagolysosomal compartment. Other bacteria such as *Legionella pneumophila*
373 have proteins such as SidK, which binds v-ATPase subunits to prevent activity (29). Our data
374 indicate that neither SLO nor any other secreted factor is responsible for interfering with v-ATPase
375 activity (Fig. 5c), and the identity of the responsible GAS protein(s) remains to be elucidated.

376 Previous data and our results indicate SLO causes leakage of lysosomal contents (Fig. 4).
377 These proteins include active lysosomal enzymes such as cathepsin B (Fig. 4) but could also include
378 bacteria proteases such as SpeB, whose presence in the cytosol could lead to NLRP3 inflammasome
379 activation and release of the proinflammatory cytokine IL-1β (46–50). Persistent IL-1β activation as
380 a result of GAS infection has been linked with ARF and rheumatic heart disease (51). Thus, besides
381 enabling bacterial survival and blunting the normal macrophage response, the resulting macrophage
382 response may lead to pathologies such as ARF that are observed during GAS infection. Furthermore,
383 SLO promotes macrophage apoptosis by releasing SLO from the lysosome and causing
384 mitochondrial damage (20,52). Loss of macrophages may also have detrimental effects on the long-
385 term response to GAS infection, including the inability to generate protective antibodies. Therapies
386 aimed at improving macrophage function may therefore improve GAS infection outcomes. Although
387 SLO is a promising target, our work shows that additional drugs to restore v-ATPase activity would
388 be necessary to restore macrophage function.

389 **5 Conflict of Interest**

The authors declare that the research was conducted in the absence of any commercial or financial relationships that could be construed as a potential conflict of interest.

6 Author Contributions

SN, JS, AT and CO contributed to conception and design of the study. All authors performed the experiments and analyzed data. CO wrote the first draft of the manuscript. All authors contributed to manuscript revision, read, and approved the submitted version.

7 Funding

Support for this project has been provided by the American Heart Association (17GRNT33410851 to CO), the Fletcher Jones Science Scholars Fellowship (to SN), the Occidental College Undergraduate Research Center (to SN, JS, JL, JS, RZ and HA), Occidental College (to CO) and the San Diego Center for Systems Biology (to AT).

8 Acknowledgments

We thank Cheldon Alcantara and Ryan Hino for contributions to experiments, and Kelvin Zheng, Jessica Kim, Stephanie Peacock, Isabel Perez, Kevin Kim, and the Fall 2021 Bio 395 GRR course for contributions to data analysis in this paper.

9 References

1. Sims Sanyahumbi A, Colquhoun S, Wyber R, Carapetis JR. Global Disease Burden of Group A Streptococcus. In: Ferretti JJ, Stevens DL, Fischetti VA, editors. Streptococcus pyogenes : Basic Biology to Clinical Manifestations [Internet]. Oklahoma City (OK): University of Oklahoma Health Sciences Center; 2016 [cited 2022 Apr 11]. Available from: http://www.ncbi.nlm.nih.gov/books/NBK333415/

2. Goldmann O, Rohde M, Chhatwal GS, Medina E. Role of Macrophages in Host Resistance to Group A Streptococci. Infect Immun. 2004 May;72(5):2956–63.

3. Mishalian I, Ordan M, Peled A, Maly A, Eichenbaum MB, Ravins M, et al. Recruited macrophages control dissemination of group A Streptococcus from infected soft tissues. J Immunol Baltim Md 1950. 2011 Dec 1;187(11):6022–31.

4. Thulin P, Johansson L, Low DE, Gan BS, Kotb M, McGeer A, et al. Viable group A streptococci in macrophages during acute soft tissue infection. PLoS Med. 2006 Mar;3(3):e53.

5. Österlund A, Popa R, Nikkilä T, Scheynius A, Engstrand L. Intracellular Reservoir of Streptococcus pyogenes In Vivo: A Possible Explanation for Recurrent Pharyngotonsillitis. The Laryngoscope. 1997;107(5):640–7.

6. Johnson AF, LaRock CN. Antibiotic Treatment, Mechanisms for Failure, and Adjunctive Therapies for Infections by Group A Streptococcus. Front Microbiol. 2021;12:760255.

7. Flannagan RS, Heit B, Heinrichs DE. Antimicrobial Mechanisms of Macrophages and the Immune Evasion Strategies of Staphylococcus aureus. Pathogens. 2015 Dec;4(4):826–68.

425 8. Carranza C, Chavez-Galan L. Several Routes to the Same Destination: Inhibition of
426 Phagosome-Lysosome Fusion by Mycobacterium tuberculosis. Am J Med Sci. 2019
427 Mar;357(3):184–94.

428 9. Misch EA. Legionella: virulence factors and host response. Curr Opin Infect Dis. 2016
429 Jun;29(3):280–6.

430 10. Ganem MB, De Marzi MC, Fernández-Lynch MJ, Jancic C, Vermeulen M, Geffner J, et al.
431 Uptake and intracellular trafficking of superantigens in dendritic cells. PloS One.
432 2013;8(6):e66244.

433 11. Siemens N, Snäll J, Svensson M, Norrby-Teglund A. Pathogenic Mechanisms of Streptococcal
434 Necrotizing Soft Tissue Infections. Adv Exp Med Biol. 2020;1294:127–50.

435 12. Staali L, Bauer S, Mörgelin M, Björck L, Tapper H. Streptococcus pyogenes bacteria modulate
436 membrane traffic in human neutrophils and selectively inhibit azurophilic granule fusion with
437 phagosomes. Cell Microbiol. 2006 Apr;8(4):690–703.

438 13. Hertzén E, Johansson L, Wallin R, Schmidt H, Kroll M, Rehn AP, et al. M1 protein-dependent
439 intracellular trafficking promotes persistence and replication of Streptococcus pyogenes in
440 macrophages. J Innate Immun. 2010;2(6):534–45.

441 14. Walker MJ, Barnett TC, McArthur JD, Cole JN, Gillen CM, Henningham A, et al. Disease
442 Manifestations and Pathogenic Mechanisms of Group A Streptococcus. Clin Microbiol Rev.
443 2014 Apr 1;27(2):264–301.

444 15. Bastiat-Sempe B, Love JF, Lomayesva N, Wessels MR. Streptolysin O and NAD-
445 glycohydrolase prevent phagolysosome acidification and promote group A Streptococcus
446 survival in macrophages. mBio. 2014 Sep 16;5(5):e01690-01614.

447 16. Bhakdi S, Tranum-Jensen J, Sziegoleit A. Mechanism of membrane damage by streptolysin-O.
448 Infect Immun. 1985 Jan;47(1):52–60.

449 17. Håkansson A, Bentley CC, Shakhnovic EA, Wessels MR. Cytolysin-dependent evasion of
450 lysosomal killing. Proc Natl Acad Sci U S A. 2005 Apr 5;102(14):5192–7.

451 18. Nordenfelt P, Grinstein S, Björck L, Tapper H. V-ATPase-mediated phagosomal acidification is
452 impaired by Streptococcus pyogenes through Mga-regulated surface proteins. Microbes Infect.
453 2012 Nov;14(14):1319–29.

454 19. Chatellier S, Ihendyane N, Kansal RG, Khambaty F, Basma H, Norrby-Teglund A, et al.
455 Genetic relatedness and superantigen expression in group A streptococcus serotype M1 isolates
456 from patients with severe and nonsevere invasive diseases. Infect Immun. 2000 Jun;68(6):3523–
457 34.

458 20. Timmer AM, Timmer JC, Pence MA, Hsu LC, Ghochani M, Frey TG, et al. Streptolysin O
459 promotes group A Streptococcus immune evasion by accelerated macrophage apoptosis. J Biol
460 Chem. 2009 Jan 9;284(2):862–71.

461 21. Lauth X, von Köckritz-Blickwede M, McNamara CW, Myskowski S, Zinkernagel AS, Beall B,
462 et al. M1 protein allows Group A streptococcal survival in phagocyte extracellular traps through
463 cathelicidin inhibition. J Innate Immun. 2009;1(3):202–14.

464 22. Datta V, Myskowski SM, Kwinn LA, Chiem DN, Varki N, Kansal RG, et al. Mutational
465 analysis of the group A streptococcal operon encoding streptolysin S and its virulence role in
466 invasive infection. Mol Microbiol. 2005 May;56(3):681–95.

467 23. Ai H wang, Olenych SG, Wong P, Davidson MW, Campbell RE. Hue-shifted monomeric
468 variants of Clavularia cyan fluorescent protein: identification of the molecular determinants of
469 color and applications in fluorescence imaging. BMC Biol. 2008 Mar 6;6:13.

470 24. Zhou C, Zhong W, Zhou J, Sheng F, Fang Z, Wei Y, et al. Monitoring autophagic flux by an
471 improved tandem fluorescent-tagged LC3 (mTagRFP-mWasabi-LC3) reveals that high-dose
472 rapamycin impairs autophagic flux in cancer cells. Autophagy. 2012 Aug;8(8):1215–26.

473 25. Jeng A, Sakota V, Li Z, Datta V, Beall B, Nizet V. Molecular genetic analysis of a group A
474 Streptococcus operon encoding serum opacity factor and a novel fibronectin-binding protein,
475 SfbX. J Bacteriol. 2003 Feb;185(4):1208–17.

476 26. McQuin C, Goodman A, Chernyshev V, Kamentsky L, Cimini BA, Karhohs KW, et al.
477 CellProfiler 3.0: Next-generation image processing for biology. PLoS Biol. 2018
478 Jul;16(7):e2005970.

479 27. McGuire CM, Forgac M. Glucose starvation increases V-ATPase assembly and activity in
480 mammalian cells through AMP kinase and phosphatidylinositide 3-kinase/Akt signaling. J Biol
481 Chem. 2018 Jun 8;293(23):9113–23.

482 28. Repnik U, Borg Distefano M, Speth MT, Ng MYW, Progida C, Hoflack B, et al. L-leucyl-L-
483 leucine methyl ester does not release cysteine cathepsins to the cytosol but inactivates them in
484 transiently permeabilized lysosomes. J Cell Sci. 2017 Sep 15;130(18):3124–40.

485 29. Xu L, Shen X, Bryan A, Banga S, Swanson MS, Luo ZQ. Inhibition of host vacuolar H+-
486 ATPase activity by a Legionella pneumophila effector. PLoS Pathog. 2010 Mar
487 19;6(3):e1000822.

488 30. Sprouffske K, Wagner A. Growthcurver: an R package for obtaining interpretable metrics from
489 microbial growth curves. BMC Bioinformatics. 2016 Apr 19;17:172.

490 31. O'Neill AM, Thurston TLM, Holden DW. Cytosolic Replication of Group A Streptococcus in
491 Human Macrophages. mBio. 2016 Apr 12;7(2):e00020-00016.

492 32. Bright NA, Davis LJ, Luzio JP. Endolysosomes Are the Principal Intracellular Sites of Acid
493 Hydrolase Activity. Curr Biol CB. 2016 Sep 12;26(17):2233–45.

494 33. Canton J, Grinstein S. Chapter 5 - Measuring lysosomal pH by fluorescence microscopy. In:
495 Platt F, Platt N, editors. Methods in Cell Biology [Internet]. Academic Press; 2015 [cited 2021
496 Jul 1]. p. 85–99. (Lysosomes and Lysosomal Diseases; vol. 126). Available from:
497 https://www.sciencedirect.com/science/article/pii/S0091679X14000223

498 34. Degnan BA, Fontaine MC, Doebereiner AH, Lee JJ, Mastroeni P, Dougan G, et al.
499 Characterization of an isogenic mutant of Streptococcus pyogenes Manfredo lacking the ability
500 to make streptococcal acid glycoprotein. Infect Immun. 2000 May;68(5):2441–8.

501 35. Cusumano ZT, Caparon MG. Citrulline protects Streptococcus pyogenes from acid stress using
502 the arginine deiminase pathway and the F1Fo-ATPase. J Bacteriol. 2015 Apr;197(7):1288–96.

503 36. Maudsdotter L, Jonsson H, Roos S, Jonsson AB. Lactobacilli reduce cell cytotoxicity caused by
504 Streptococcus pyogenes by producing lactic acid that degrades the toxic component lipoteichoic
505 acid. Antimicrob Agents Chemother. 2011 Apr;55(4):1622–8.

506 37. Daglia M, Papetti A, Grisoli P, Aceti C, Dacarro C, Gazzani G. Antibacterial activity of red and
507 white wine against oral streptococci. J Agric Food Chem. 2007 Jun 27;55(13):5038–42.

508 38. Jin H, Agarwal S, Agarwal S, Pancholi V. Surface export of GAPDH/SDH, a glycolytic
509 enzyme, is essential for Streptococcus pyogenes virulence. mBio. 2011;2(3):e00068-00011.

510 39. Cotter PD, Hill C. Surviving the acid test: responses of gram-positive bacteria to low pH.
511 Microbiol Mol Biol Rev MMBR. 2003 Sep;67(3):429–53, table of contents.

512 40. Molloy EM, Cotter PD, Hill C, Mitchell DA, Ross RP. Streptolysin S-like virulence factors: the
513 continuing sagA. Nat Rev Microbiol. 2011 Sep;9(9):670–81.

514 41. Shaughnessy LM, Hoppe AD, Christensen KA, Swanson JA. Membrane perforations inhibit
515 lysosome fusion by altering pH and calcium in Listeria monocytogenes vacuoles. Cell
516 Microbiol. 2006 May;8(5):781–92.

517 42. Ambati J, Canakis CS, Miller JW, Gragoudas ES, Edwards A, Weissgold DJ, et al. Diffusion of
518 high molecular weight compounds through sclera. Invest Ophthalmol Vis Sci. 2000
519 Apr;41(5):1181–5.

520 43. Cheng YL, Wu YW, Kuo CF, Lu SL, Liu FT, Anderson R, et al. Galectin-3 Inhibits Galectin-
521 8/Parkin-Mediated Ubiquitination of Group A Streptococcus. mBio. 2017 Jul 25;8(4):e00899-
522 17.

523 44. O'Seaghdha M, Wessels MR. Streptolysin O and its co-toxin NAD-glycohydrolase protect
524 group A Streptococcus from Xenophagic killing. PLoS Pathog. 2013;9(6):e1003394.

525 45. Cusumano ZT, Watson ME, Caparon MG. Streptococcus pyogenes arginine and citrulline
526 catabolism promotes infection and modulates innate immunity. Infect Immun. 2014
527 Jan;82(1):233–42.

528 46. Keyel PA, Roth R, Yokoyama WM, Heuser JE, Salter RD. Reduction of streptolysin O (SLO)
529 pore-forming activity enhances inflammasome activation. Toxins. 2013 Jun 6;5(6):1105–18.

530 47. Chu J, Thomas LM, Watkins SC, Franchi L, Núñez G, Salter RD. Cholesterol-dependent
531 cytolysins induce rapid release of mature IL-1beta from murine macrophages in a NLRP3
532 inflammasome and cathepsin B-dependent manner. J Leukoc Biol. 2009 Nov;86(5):1227–38.

533 48. Richter J, Monteleone MM, Cork AJ, Barnett TC, Nizet V, Brouwer S, et al. Streptolysins are
534 the primary inflammasome activators in macrophages during Streptococcus pyogenes infection.
535 Immunol Cell Biol. 2021 Nov;99(10):1040–52.

536 49. LaRock DL, Russell R, Johnson AF, Wilde S, LaRock CN. Group A Streptococcus Infection of
537 the Nasopharynx Requires Proinflammatory Signaling through the Interleukin-1 Receptor.
538 Infect Immun. 2020 Sep 18;88(10):e00356-20.

539 50. Campden RI, Zhang Y. The role of lysosomal cysteine cathepsins in NLRP3 inflammasome
540 activation. Arch Biochem Biophys. 2019 Jul 30;670:32–42.

541 51. Kim ML, Martin WJ, Minigo G, Keeble JL, Garnham AL, Pacini G, et al. Dysregulated IL-1β-
542 GM-CSF Axis in Acute Rheumatic Fever That Is Limited by Hydroxychloroquine. Circulation.
543 2018 Dec 4;138(23):2648–61.

544 52. Cortés G, Wessels MR. Inhibition of dendritic cell maturation by group A Streptococcus. J
545 Infect Dis. 2009 Oct 1;200(7):1152–61.

546

547 **10 Tables**

548 **Table 1: Final pH of media after bacterial growth, mean ± SD**

starting pH	4.0	5.0	6.0	7.0	media (6.6)
ending pH	4.10 ± 0.02	5.07 ± 0.02	4.99 ± 0.01	5.23 ± 0.08	5.63 ± 0.06

549 **11 Figure legends**

550 **Figure 1: GAS persists in phagolysosomes of THP-1 cells.** THP-1 cells were infected with GAS
551 for the indicated times, fixed and probed with anti-LAMP-1 (green) and anti-human IgG (bacteria,
552 red) antibodies. **(A)** Representative image of LAMP-1 colocalized with GAS in THP-1 cells at 60
553 min. post-infection. Arrowheads indicate examples of colocalization. **(B)** Quantitation of LAMP-1
554 positive bacteria at the indicated time points. **(C)** Average number of bacteria per cell at the indicated
555 time points. For all graphs, data from three independent experiments were combined and results are
556 given as mean ± 95% CI. Data were analyzed by one-way ANOVA with Tukey's multiple
557 comparisons test.

558 **Figure 2: GAS persists in non-acidified phagolysosomes of THP-1 cells. (A)** GAS expressing
559 mWASABI were incubated at the indicated pH. Representative green fluorescence (mWASABI) and
560 brightfield images are shown. **(B)** Corrected total cell fluorescence of green fluorescence signal from
561 bacteria expressing mWASABI incubated at the indicated pH for 1 hour. **(C)** Representative
562 fluorescence microscopy images of GAS-infected THP-1 cells at 7.5 and 60 min. post-infection.
563 Arrowheads denote examples of bacteria encapsulated in early phagosomes (EEA-1, magenta),
564 arrows denote examples of bacteria encapsulated in phagolysosomes (LAMP-2, red). Fluorescence

565 images merged with brightfield images are shown in the bottom row. All images were taken with a
566 63x objective with 2x digital zoom. **(D)** Quantitation of bacteria colocalized with phagosomes (EEA-
567 1) or phagolysosomes (LAMP-2) at the indicated time points. **(E)** Average number of bacteria per
568 cell at the indicated time points. **(F)** Violin plot of fluorescence signal intensity from intracellular
569 (clear bars) or extracellular (shaded bars) bacteria expressing mWASABI. **(G)** Fluorescence signal
570 from cells fed 70kD FITC dextran and infected with immunoglobulin-conjugated beads (Ab beads),
571 the indicated GAS strain or heat-killed (HK) bacteria. Significance indicates difference from Ab
572 beads (positive control). Data from at least three independent experiments were combined. For (D)
573 and (E), data from 5 individual counters of three independent experiments were combined. Results
574 are given as mean ± 95% CI and analyzed by one-way ANOVA with Kruskal-Wallis multiple
575 comparison test.

576 **Figure 3: GAS does not survive in low pH environments. (A)** Growth curves of bacteria grown in
577 buffered media or unbuffered bacterial media (THB) at the indicated pH. Results are given as mean ±
578 95% CI. Statistics in (A) indicate differences in intrinsic growth rate compared with bacteria grown
579 in unbuffered media. **(B)** Bacterial survival in buffered media at the indicated pH compared with
580 survival of bacteria in unbuffered bacterial media (THB). Results are given as mean ± SEM.
581 Statistics in (B) are shown only for pH = 4.9 and 5.3 media and indicate differences in bacterial
582 survival at the corresponding time point compared with bacteria in unbuffered media. Differences for
583 bacteria grown in pH = 4.7 or lower media were statistically significant compared with unbuffered
584 media at all time points after 30 min. For each experiment, samples were prepared in triplicate and
585 data from at least three independent experiments were combined.

586 **Figure 4: SLO induces phagolysosomal perforation and protein leakage. (A)** Representative
587 images of the 40kD dextran probe (green) with indicated bacterial strains (magenta). Arrowheads
588 indicate examples of colocalization. All images were taken with a 63x objective with 2x digital
589 zoom. **(B)** Quantitation of colocalization of indicated bacterial strains with 10, 40 and 70kD dextran
590 probes. Results are given as mean ± 95% CI and analyzed by one-way ANOVA with Tukey's
591 multiple comparison test. **(C)** Cells were infected with the indicated bacterial strains, fractionated
592 into membrane (left) and cytosolic (right) fractions, and probed with the indicated antibodies:
593 LAMP-2 (lysosomal marker; loading control for membrane fraction), GAPDH (cytosolic marker;
594 loading control for cytosolic fraction) and cathepsin B (lysosomal enzyme). **(D)** Cathepsin B activity
595 was measured in cytosolic cell fractions collected from cells infected with the indicated strains. Data
596 in (B) and (D) are combined from at least three independent experiments.

597 **Figure 5: GAS infection limits v-ATPase activity. (A)** Cells were infected with immunoglobulin-
598 conjugated beads (Ab beads, control), the indicated GAS strain or heat-killed (HK) bacteria and
599 fractionated into membrane (M) and cytosolic (C) fractions. Fractions were probed with antibodies to
600 V_1A, V_0D or GAPDH proteins. Representative data are shown. **(B)** Quantitation of data shown in
601 (A). V_1A band intensities were quantified and normalized to V_0D (membrane) or GAPDH (cytosol).
602 Relative assembly was calculated as the amount of V_1A in the membrane fraction of the indicated
603 infected sample compared with the uninfected sample for each experiment. **(C)** v-ATPase activity
604 assay in membrane fractions from cells infected with the indicated GAS strain. Data in (B) and (C)
605 are combined from at least three independent experiments and results are given as mean ± 95% CI
606 and analyzed by one-way ANOVA with Tukey's multiple comparison test.

A

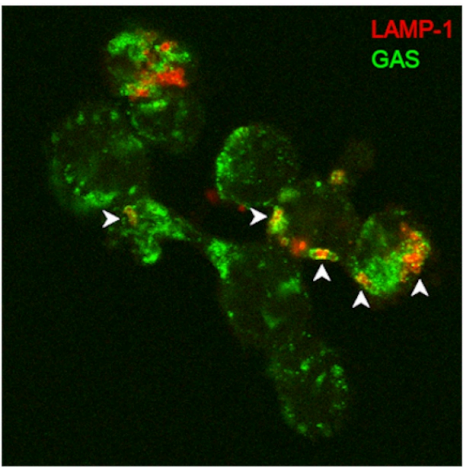
LAMP-1
GAS

B

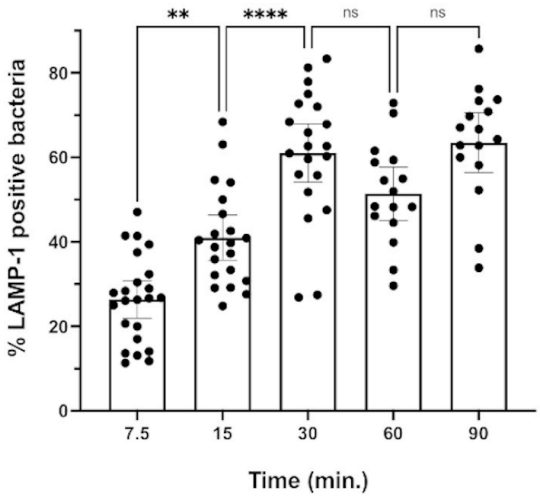
**
****
ns
ns
% LAMP-1 positive bacteria
0
20
40
60
80
7.5
15
30
60
90
Time (min.)

C

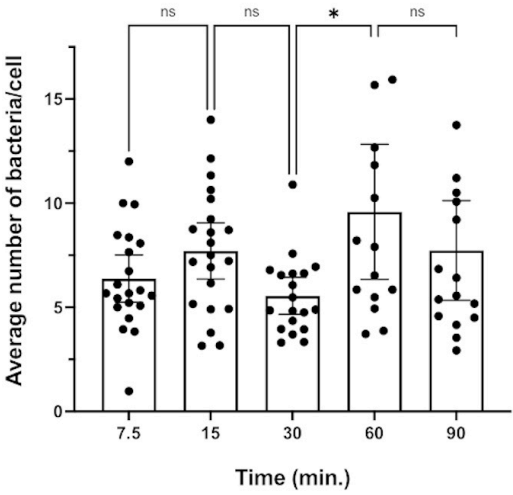
ns
ns
*
ns
Average number of bacteria/cell
0
5
10
15
7.5
15
30
60
90
Time (min.)

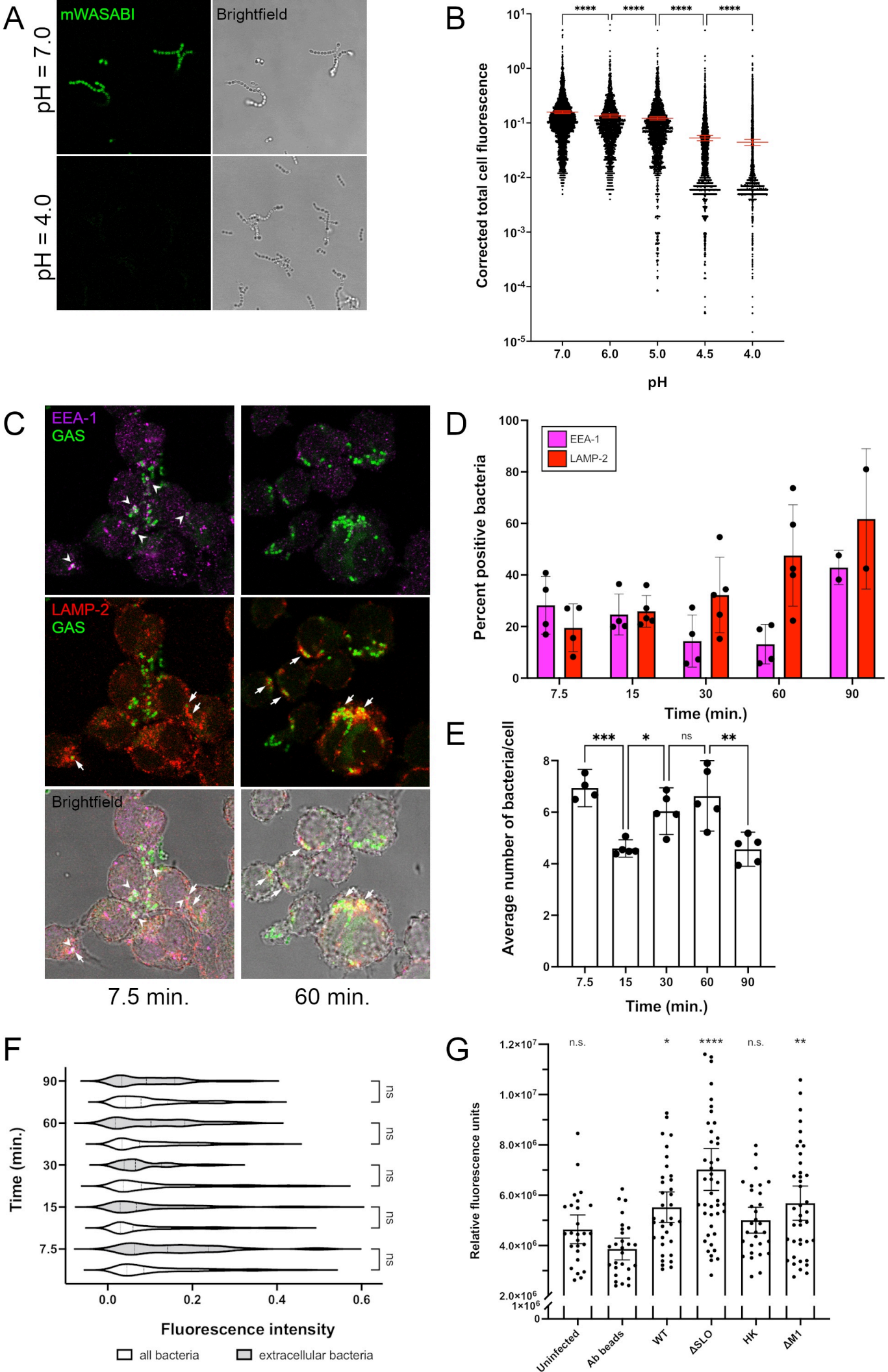
A
mWASABI
Brightfield
pH = 7.0
pH = 4.0
B
Corrected total cell fluorescence
pH
7.0
6.0
5.0
4.5
4.0
****
C
EEA-1
GAS
LAMP-2
GAS
Brightfield
7.5 min.
60 min.
D
EEA-1
LAMP-2
Percent positive bacteria
Time (min.)
E
Average number of bacteria/cell
Time (min.)
***
*
ns
**
F
Time (min.)
Fluorescence intensity
all bacteria
extracellular bacteria
ns
G
Relative fluorescence units
n.s.
*
****
n.s.
**
Uninfected
Ab beads
WT
ΔSLO
HK
ΔM1

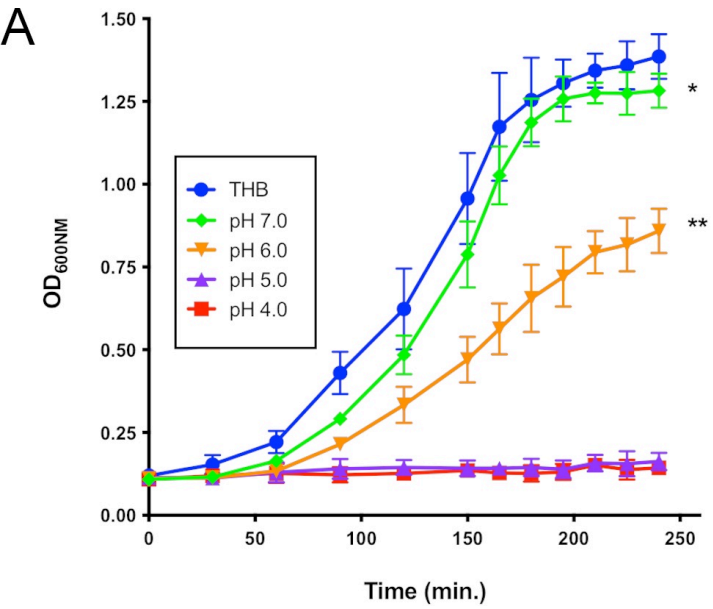
A
1.50
1.25
1.00
0.75
0.50
0.25
0.00
OD600NM
0
50
100
150
200
250
Time (min.)
THB
pH 7.0
pH 6.0
pH 5.0
pH 4.0
*
**

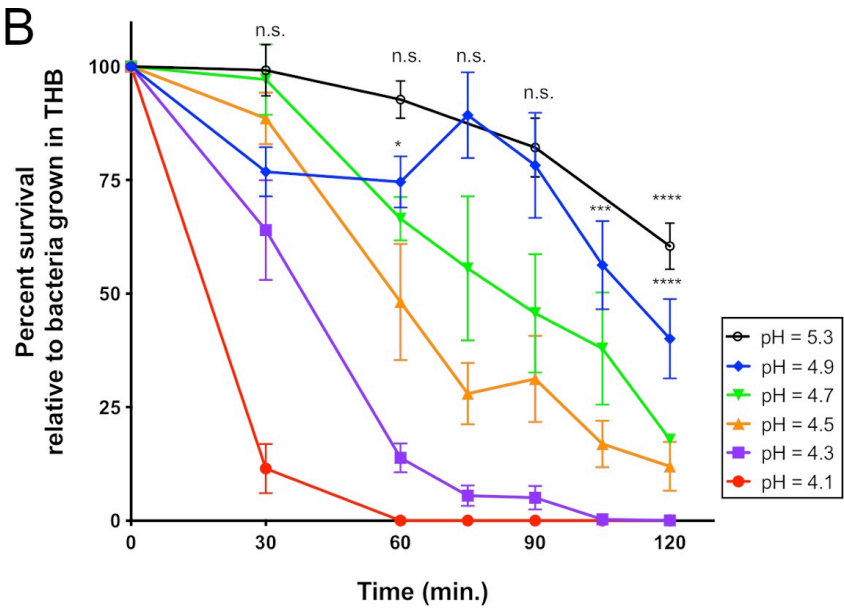
B
Percent survival
relative to bacteria grown in THB
100
75
50
25
0
0
30
60
90
120
Time (min.)
n.s.
n.s.
n.s.
n.s.
*
***
****
****
pH = 5.3
pH = 4.9
pH = 4.7
pH = 4.5
pH = 4.3
pH = 4.1

A

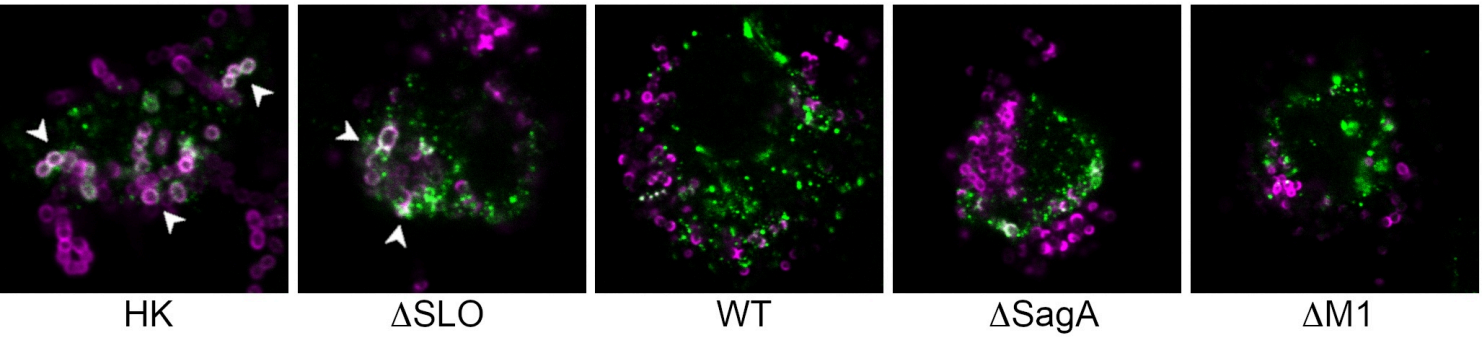
HK
ΔSLO
WT
ΔSagA
ΔM1

B

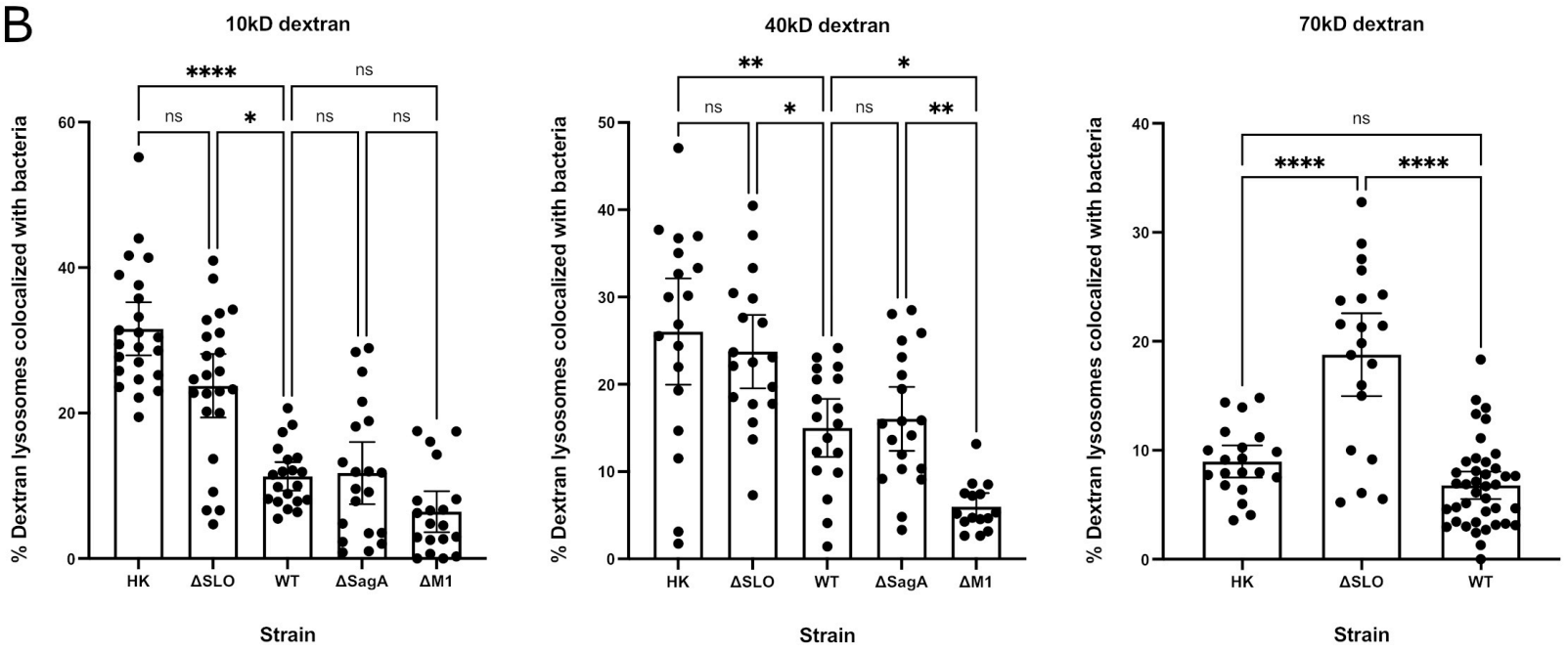
10kD dextran
40kD dextran
70kD dextran
% Dextran lysosomes colocalized with bacteria
Strain
HK
ΔSLO
WT
ΔSagA
ΔM1
ns
*
**
****

C

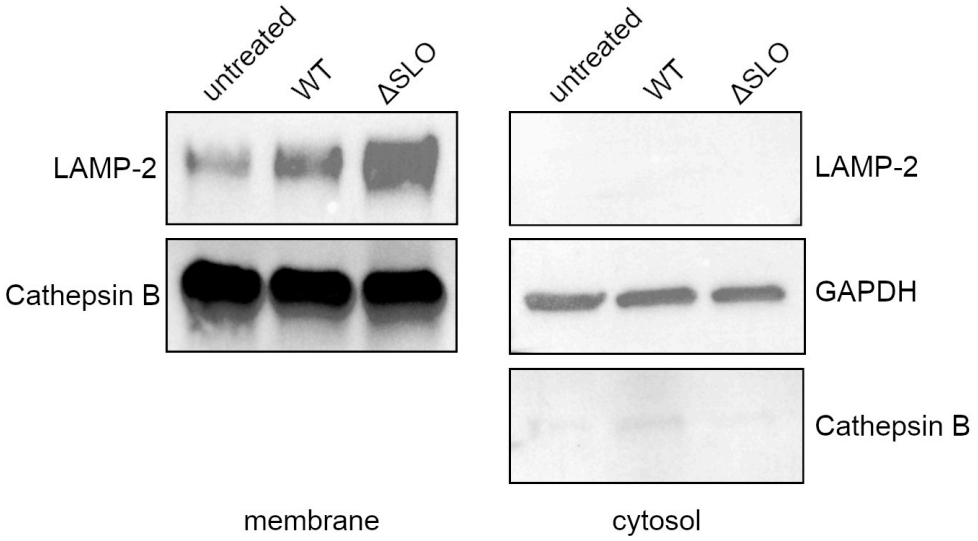
untreated
WT
ΔSLO
LAMP-2
Cathepsin B
GAPDH
membrane
cytosol

D

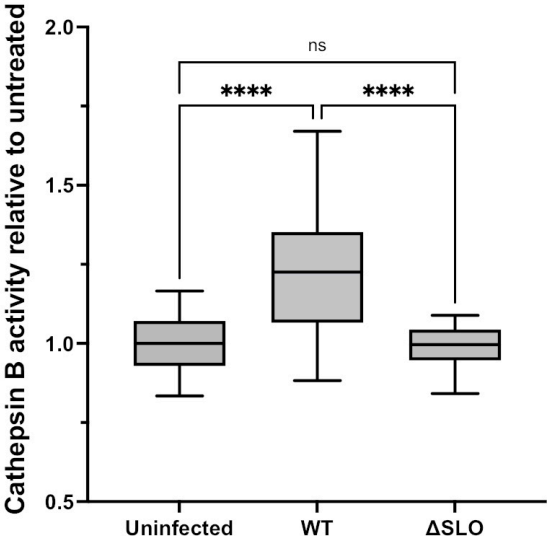
Cathepsin B activity relative to untreated
Uninfected
WT
ΔSLO
ns
****

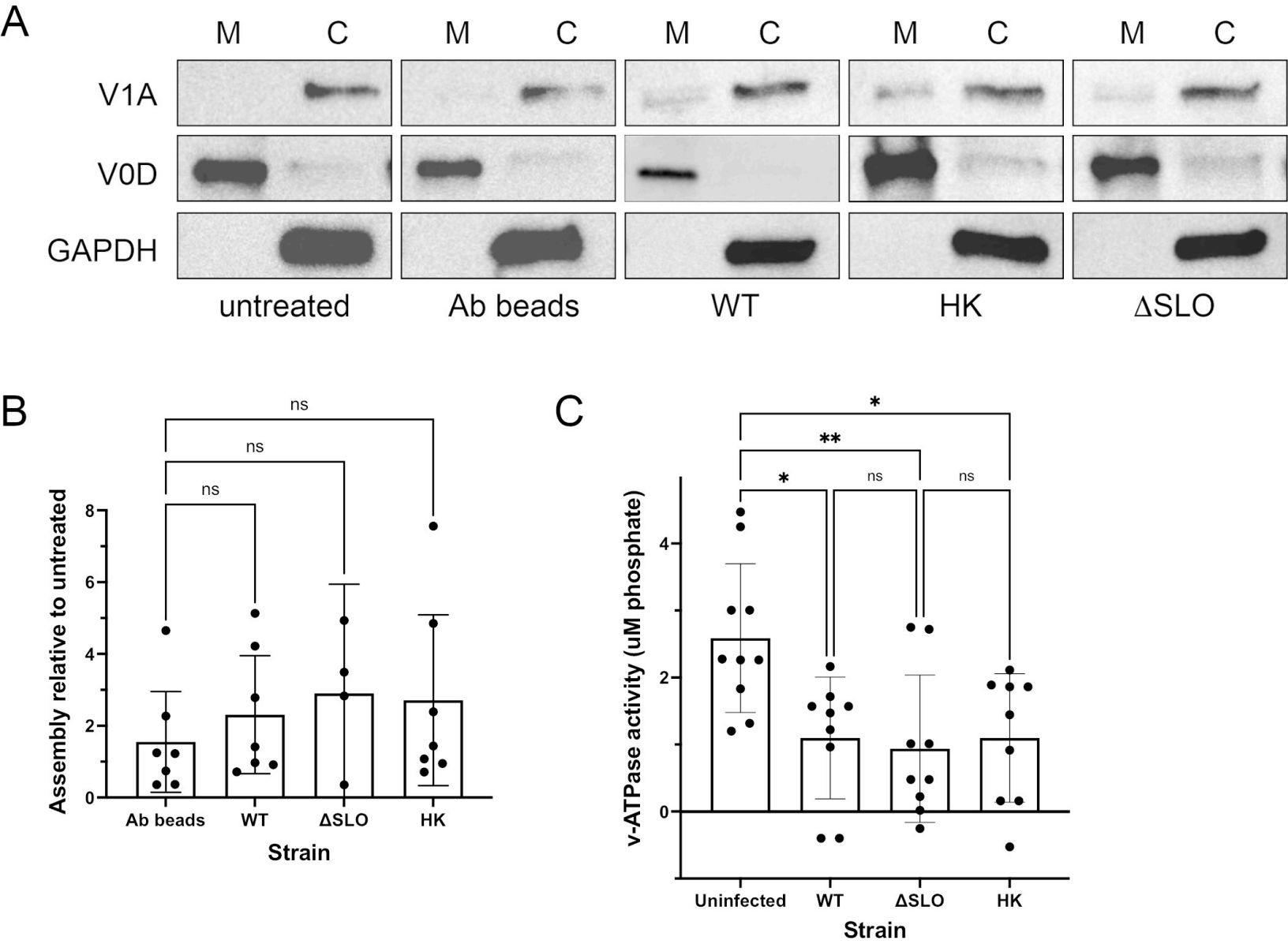
A
M
C
V1A
V0D
GAPDH
untreated
Ab beads
WT
HK
ΔSLO
B
ns
Assembly relative to untreated
Ab beads
WT
ΔSLO
HK
Strain
C
*
**
ns
v-ATPase activity (uM phosphate)
Uninfected
Strain

Supplementary Material

1 Supplementary Data

mWASABI amino acid sequence:

MVSKGEETTMGVIKPDMKIKLKMEGNVNGHAFVIEGEGEGKPYDGTNTINLEVKEGAPLPF
SYDILTTAFSYGNRAFTKYPDDIPNYFKQSFPEGYSWERTMTFEDKGIVKVKSDISMEEDSFI
YEIHLKGENFPPNGPVMQKETTGWDASTERMYVRDGVLKGDVKMKLLLEGGGHHRVDFK
TIYRAKKAVKLPDYHFVDHRIEILNHDKDYNKVTVYEIAVARNSTDGMDELYK

2 Supplementary Figures

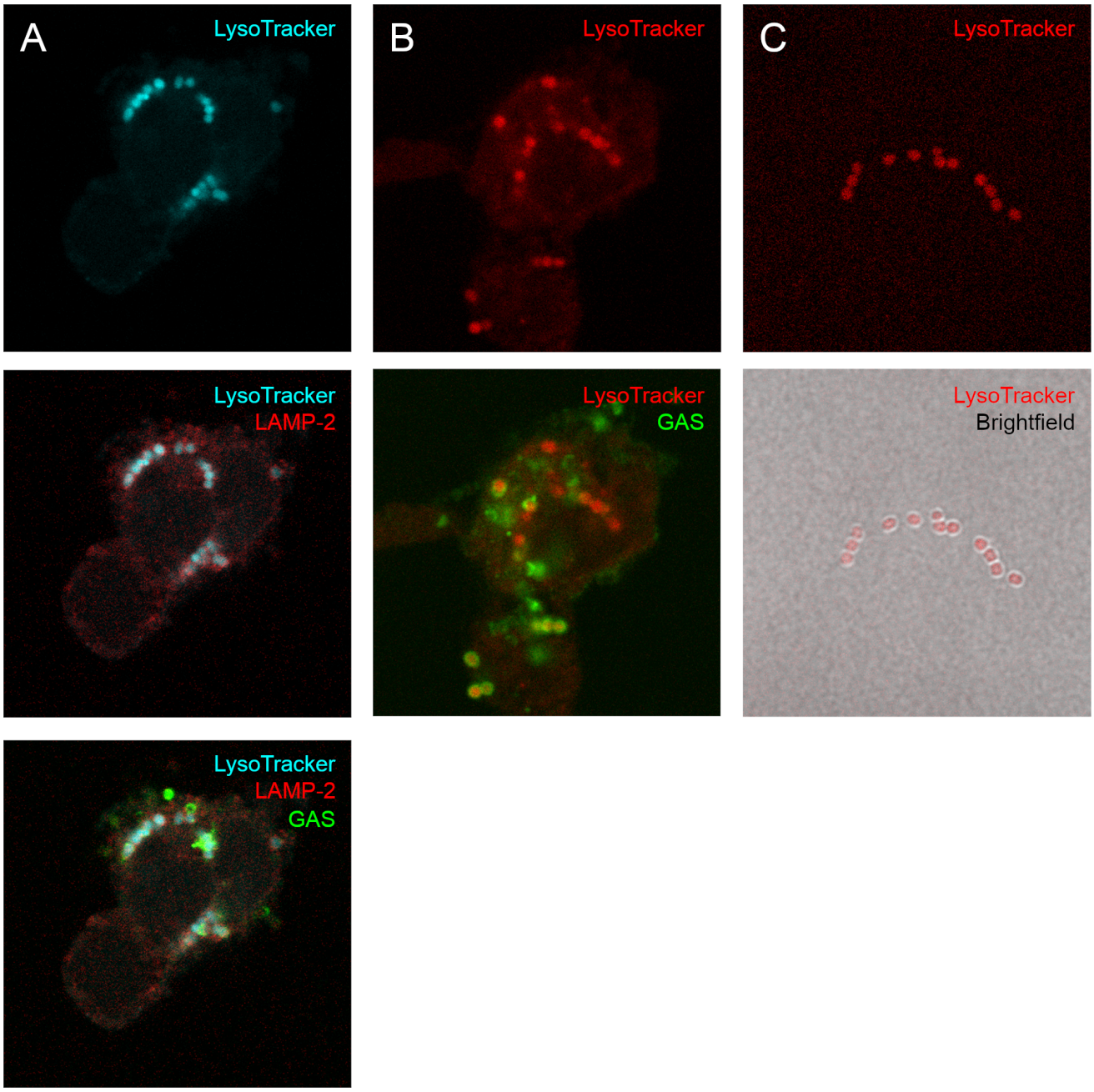

Supplemental Figure 1: Lysotracker detects GAS. Cells were loaded with 100nM LysoTracker Deep Red (Thermo Fisher Scientific) prior to infection and infected with GAS for 30 min. Cells were fixed and stained with LAMP-2 (lysosome) and anti-human IgG (bacteria) antibodies as indicated: **(A)** LysoTracker (blue), LAMP-2 (red), and GAS (green). **(B)** Lysotracker (red) and GAS (green). **(C)** Bacteria alone incubated with 100nM Lysotracker (red). All images were taken with a 63x objective with 2x digital zoom.

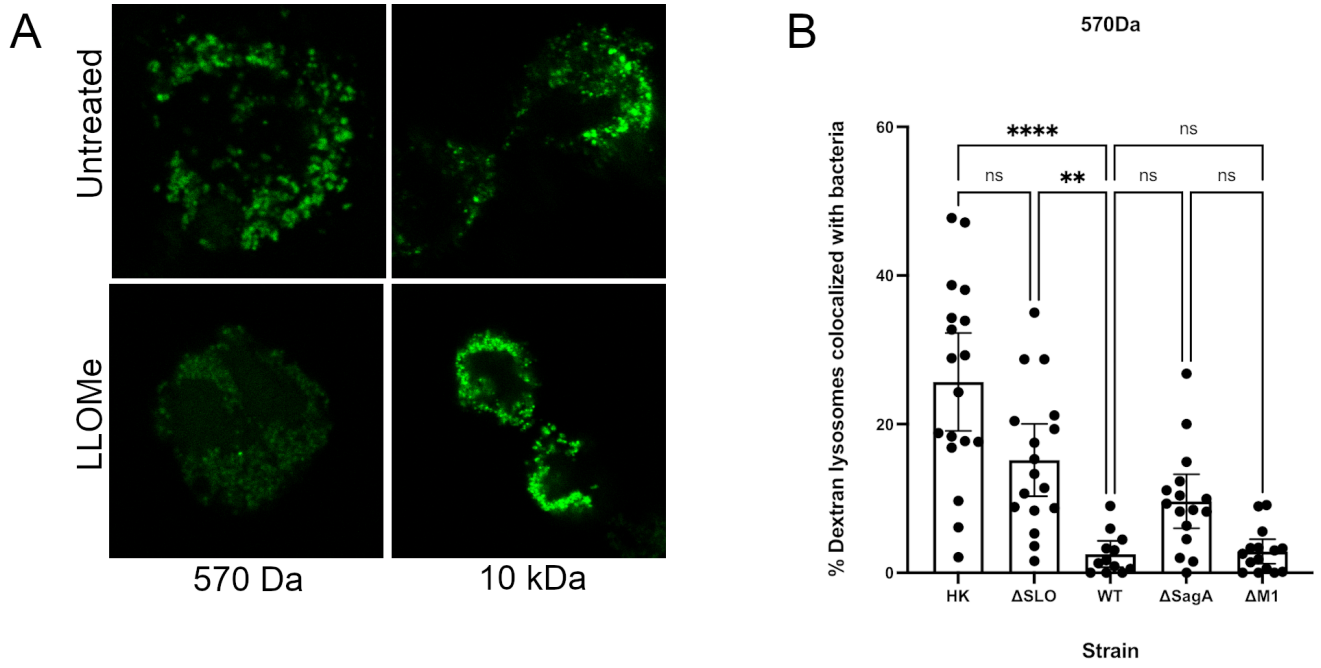

Supplemental Figure 2: Fluorescent probes appropriately monitor phagolysosomal leakage. Cells were loaded with Alexa-fluor 488 dye (570 Da) or 10kD Oregon Green dextran (10kDa) for 24 hrs., then either untreated, treated with 1mM LLOMe or infected with the indicated GAS strain. **(A)** Representative images of fluorescent probe-loaded cells in the presence or absence of LLOMe. All images were taken with a 63x objective with 2x digital zoom. **(B)** Quantitation of colocalization of Alexa-fluor 488 (570Da) with indicated bacterial strains. Data from three independent experiments were combined and are given as mean ± 95% CI.

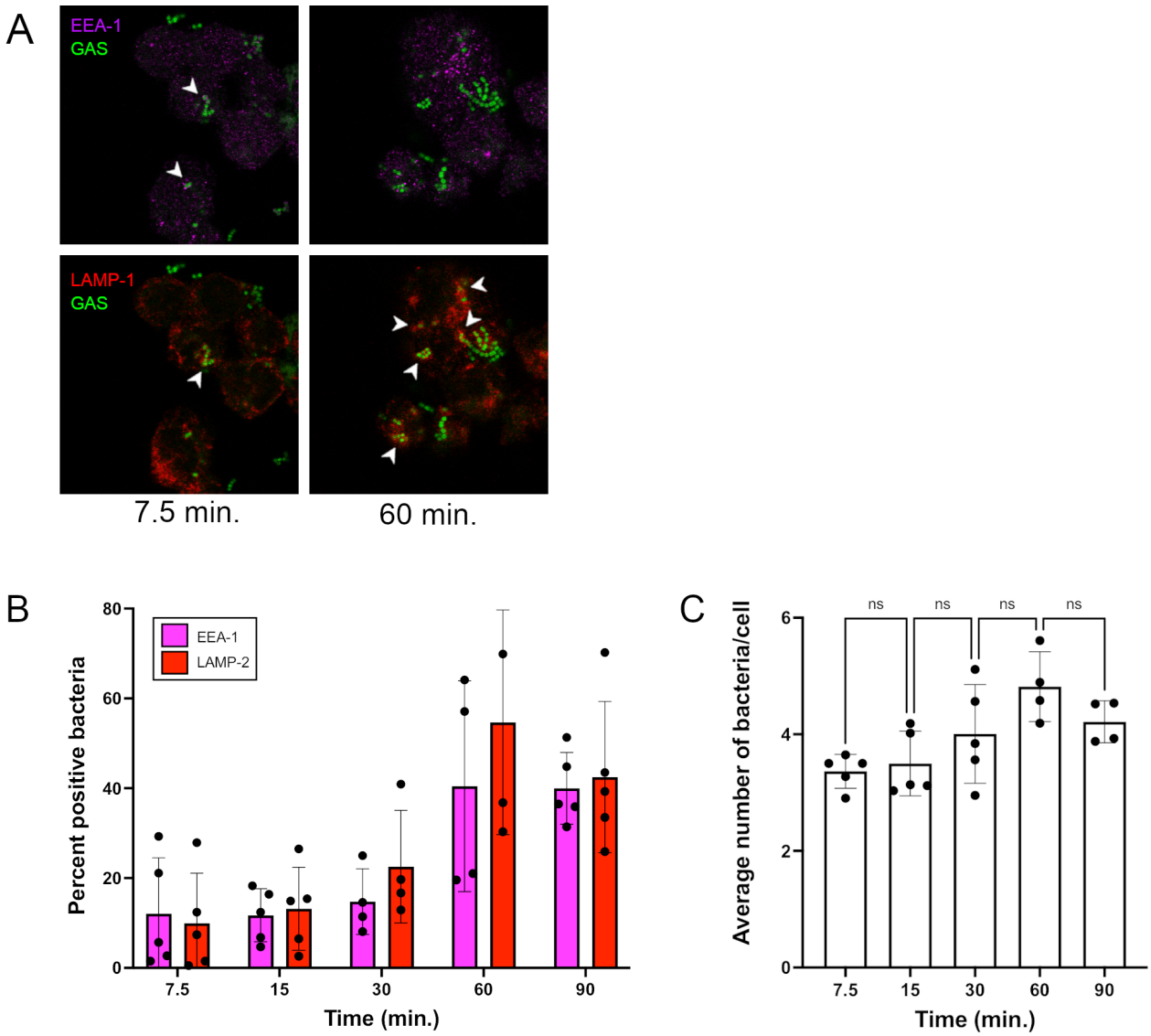

Supplemental Figure 3: ΔSLO GAS persist in THP-1 phagolysosomes. (A) Representative fluorescence microscopy images of ΔSLO-infected THP-1 cells at 7.5 and 60 min. post-infection. Arrowheads denote examples of ΔSLO bacteria (green) encapsulated in early phagosomes (EEA-1, magenta) or in phagolysosomes (LAMP-2, red). All images were taken with a 63x objective with 2x digital zoom. **(B)** Quantitation of bacteria in intracellular compartments. **(C)** Average number of bacteria per cell at the indicated time points. For B and C, data from at least 5 individual counters of three independent experiments were combined. Results are given as mean ± 95% CI and analyzed by one-way ANOVA with Kruskal-Wallis multiple comparison test.